Supporting Information

Electrochemical Hydrogenation of a Homogeneous Nickel Complex to a Form a Surface Adsorbed Hydrogen-Evolving Species

Daniel J. Martin,[a] Brian D. McCarthy,[a] Carrie L. Donley,[b] and Jillian L. Dempsey[a]*

[a]Department of Chemistry and [b]Chapel Hill Analytical and Nanofabrication Laboratory,
Department of Applied Physical Sciences

University of North Carolina Chapel Hill, North Carolina 27599-3216, United States

email: dempseyj@email.unc.edu

Index *Page*

General experimental

Syntheses were performed either in a nitrogen filled glovebox or on a high-vacuum manifold. Acetonitrile (Fischer Scientific, HPLC grade, >99.9%) was dried and degassed with argon using a Pure Process Technology solvent system. 2-aminothiophenol (Alfa Aesar, 98%), 2-pyridinecarboxaldehyde (Alpha Aesar, 99%) nickel perchlorate hexahydrate (Sigma-Aldrich), nickel acetate tetrahydrate (Sigma-Aldrich, >98%), methyl iodide (Fisher Scientific), sodium borohydride (Aldrich, >99%) sodium tetrafluoroborate (Aldrich, 98%), 2-(methylthioaniline) (Acros Organics, >97%), water for polishing (Fisher Scientific, HPLC grade), magnesium sulfate (Sigma Aldrich, >99.5%), sodium chloride (Aldrich, >99%), diethyl ether (Fisher, >99.0%), ethanol (Decon Labs, Inc., 200 proof), methanol (Fisher, >99.9%), deuterated acetone (Cambridge Isotope Labs, Inc., >99.8%), deuterated chloroform (Cambridge Isotope Labs, Inc., 99.8%) were all used as received. Trifluoroacetic acid (Sigma-Aldrich, 99%) was degassed with three freeze-pump-thaw cycles. Tetrabutylammonium hexafluorophosphate (TCI, >98%) was recrystallized from hot ethanol, filtered, washed with cold ethanol, and dried at room temperature under vacuum for 19 hours. 2-Pyridyl-N-(2’-thiolophenyl)methyleneimine,[1] bis(2-pyridyl-N-(2’-thiolophenyl)methylenimine)nickel(II),[2] 2-Pyridyl-N-(2’-methylthiophenyl)methyleneimine,[3] 2-Pyridyl-N-(2’-methylthiophenyl)methylamine,[3] and bis(2-pyridyl-N- (2’-methylthio phenyl)methylamine)nickel(II) perchlorate (**2**),[3] were prepared by literature methods.

NMR spectra were recorded on a Bruker 400 MHz spectrometer and referenced to proteo solvent impurities.[4] Atlantic Microlabs, Inc. performed all elemental analysis. UV-vis spectra were recorded in a nitrogen filled glovebox using fiber optic cables connected to an Agilent Cary 60 UV-vis spectrophotometer. X-ray photoelectron spectra were recorded using a Kratos Axis Ultra DLD X-ray Photoelectron Spectrometer. Spectra were obtained with a monochromatic Al Kα X-ray source, and survey and high resolution scans were obtained with pass energies of 80 and 20 eV, respectively. Scanning electron microscopy (SEM) was performed using a Hitachi S4700 FESEM and EDS obtained using Oxford INCA PentaFETx3. SEM analysis was done using 20 kV accelerating voltage and close to 12 mm working distance. Transmission electron microscopy (TEM) was performed using a JEOL 2010F FasTEM and EDS obtained using an Oxford INCA Energy 250. TEM analysis was done using 200 kV accelerating voltage. TEM samples were prepared by scraping a small amount of electrodeposited sample from the glassy carbon substrate and dispersing it in ethanol via ultrasonication. An aliquot of the sample was drop cast on a copper Formvar TEM grid.

Electrochemical methods

Electrochemistry was performed in a nitrogen filled glovebox with a Pine Instruments WaveDriver potentiostat using glassy carbon working electrodes, a glassy carbon counter electrode, and a silver wire pseudoreference. Leads for the WaveDriver potentiostat were connected to an external computer via a custom feedthrough in the back of the glovebox. All scans were absolutely referenced to ferrocene added at the end of each measurement set. Glassy carbon electrodes (CH Instruments, 3 mm diameter) were polished with 0.3 micron alumina powder and 0.05 micron alumina powder (CH Instruments, contained no agglomerating agents) Milli-Q water slurries, rinsed and ultrasonicated for one minute in HPLC water to remove residual polishing powder. The pseudoreference silver wire electrode was submerged in a glass tube fitted with a porous glass Vycor tip containing 100 mM [Bu_4N][PF_6] in acetonitrile.

Each working electrode was pretreated with three cyclical scans from approximately 0.7 V to –2.8 V (the exact value varied with the silver wire pseudoreference) at 100 mV/s in 0.1 M [Bu_4N][PF_6]. For all experiments, background voltammograms at the respective scan rate were taken. The solution was stirred between scans. For each scan, a fresh, pretreated working electrode was used unless otherwise noted.

Surface analysis sample preparation

Dropcast samples of [Bu_4N][PF_6], **1**, **2** were all prepared on unmodified gold plated silica wafers provided by Chapel Hill Analytical Nanofabrication Laboratory (CHANL).

Electrolyzed samples of **1** and **2** were prepared as follows. Glassy carbon plates (1 x 1 cm, 1 mm thickness, ALS-Japan), were polished by a multistep process. Each was first polished using 0.05 micron alumina powder (CH Instruments, contained no agglomerating agents) Milli-Q water slurries, rinsed and ultrasonicated for one minute in HPLC water to remove residual polishing powder. This process was repeated for each plate. Finally, each plate was given a third polishing using a new polishing pad, followed by sonication and drying. Electrolyzed samples were produced using a compartmentalized electrochemical cell in which the counter, reference, and working plates were separated by porous frits. To solutions of the respective complexes and acid, a potential (as noted for each sample) was applied for eight minutes under pseudo steady state conditions (constant stirring of the solution in the main compartment). After electrolysis, samples were removed from the solutions, blotted dry, and placed under vacuum for 30 minutes. XPS samples were transferred to the instrument under N_2 using a N_2 glovebag. SEM samples were briefly exposed to the atmosphere while loading.

Synthesis and characterization of 1

Bis(2-pyridyl-N-(2'-methylthiophenyl)methylenimine)nickel(II) tetrafluoroborate (**1**). $NaBF_4$ (0.40 g, 3.65 mmol, 6.30 equiv) was dissolved in 40 mL MeOH and combined in a roundbottom flask with a suspension of bis(2-pyridyl-N-(2'-thiolophenyl)methylenimine)nickel(II) (0.280 g, 0.58 mmol, 1.00 equiv) in 20 mL MeOH. The solution was heated to reflux under atmosphere before MeI (1.5 mL, 24.1 mmol, 41.6 equiv) was injected into the refluxing solution. The solution was stirred at reflux for 1 hr. before additional MeI (1.5 mL, 24.1 mmol, 41.6 equiv) was injected into the refluxing solution. The solution was further stirred at reflux for 30 minutes before it was removed from heat and cooled to room temperature. The precipitate was filtered and rinsed with 15 mL MeOH before collecting red, rust colored crude product (0.28 g). Recrystallization of the crude product from hot water yielded small red crystals. The recrystallization solvent was decanted and the crystals were rinsed with Et_2O. The crystals were further recrystallized (x3) from an acetone-water mixture (1:4) with dissolved $NaBF_4$ (0.10 g, 0.912 mmol). Between recrystallizations the solvent was decanted and the crystals were rinsed with Et_2O. The product was then recrystallized (x2) from HPLC water. The repeated recrystallizations were required to remove iodine from the sample as confirmed by elemental analysis. Finally, the recytallization solvent was decanted and the crystals were rinsed with Et_2O. Red cube-like crystals were collected and dried. Yield: 0.109 g (27.25%). Elemental analysis calculated for $C_{26}H_{24}N_4S_2B_2F_8Ni$, **1**: C 45.33; H 3.51; N 8.13. Found: C 45.17; H 3.66; N 8.07.

Ligand NMR characterization

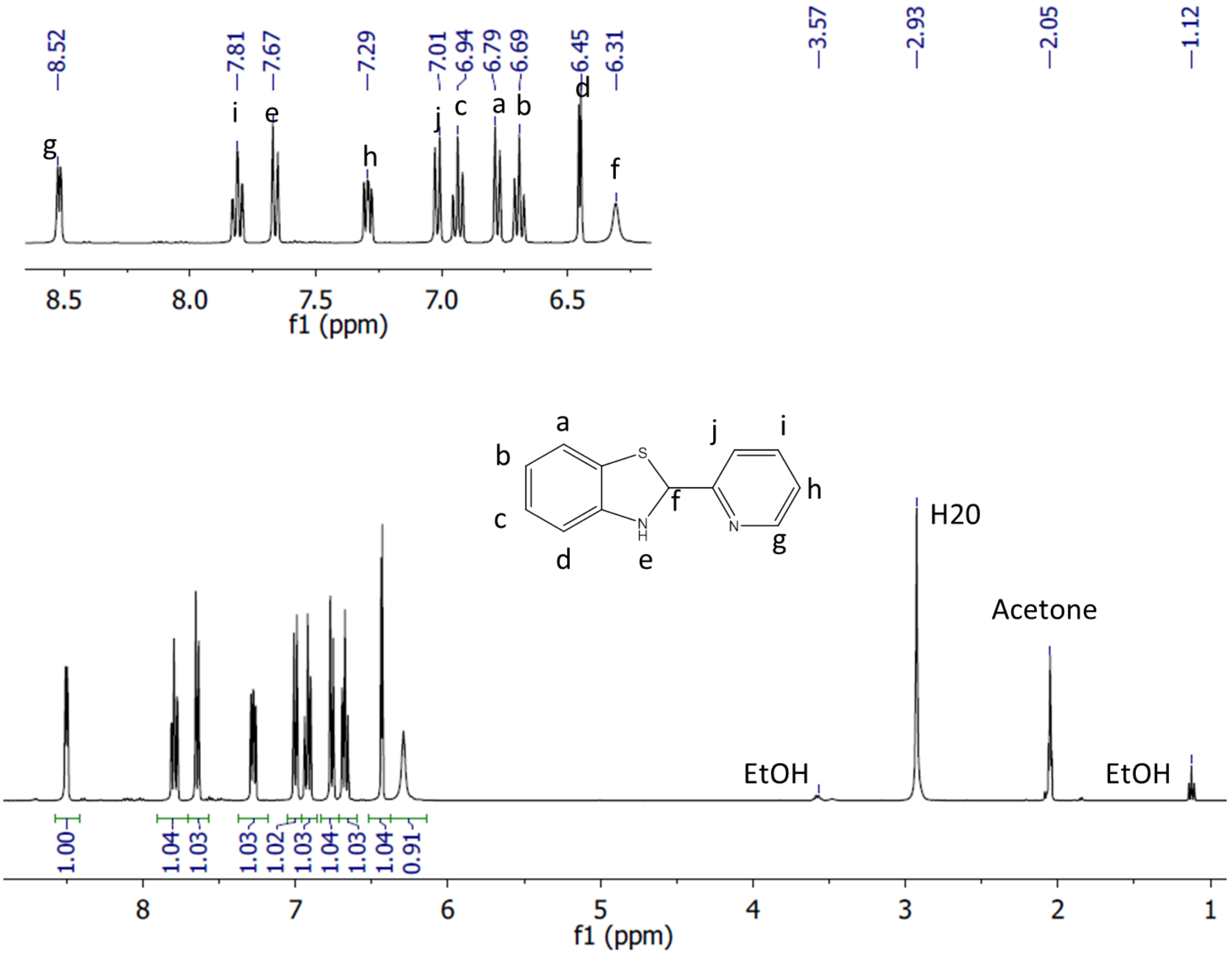

Figure S1. 2-Pyridyl-N-(2'-thiolophenyl)methyleneimine NMR spectrum in $(CD_3)_2CO$ at 400 MHz.

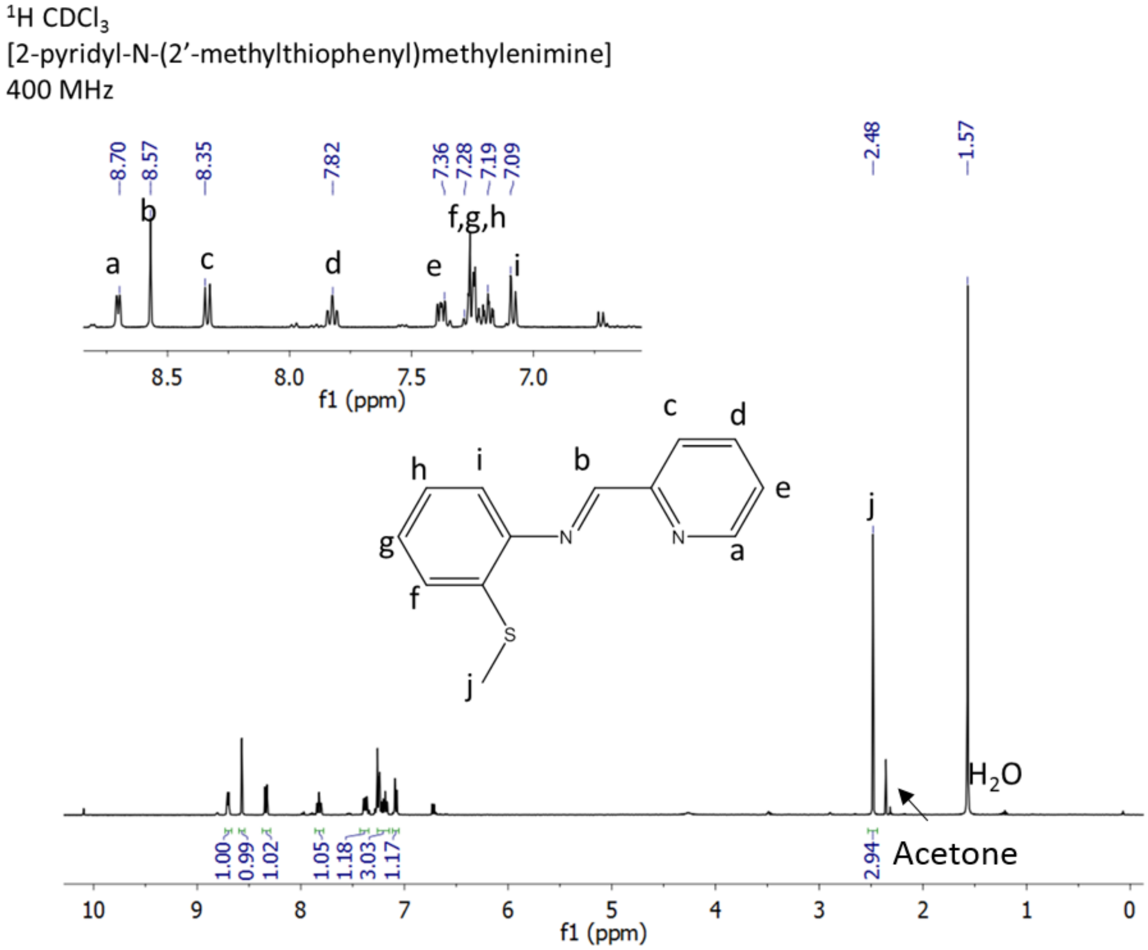

Figure S2. 2-Pyridyl-N-(2'-methylthiophenyl)methyleneimine NMR in CDCl$_3$ at 400 MHz.

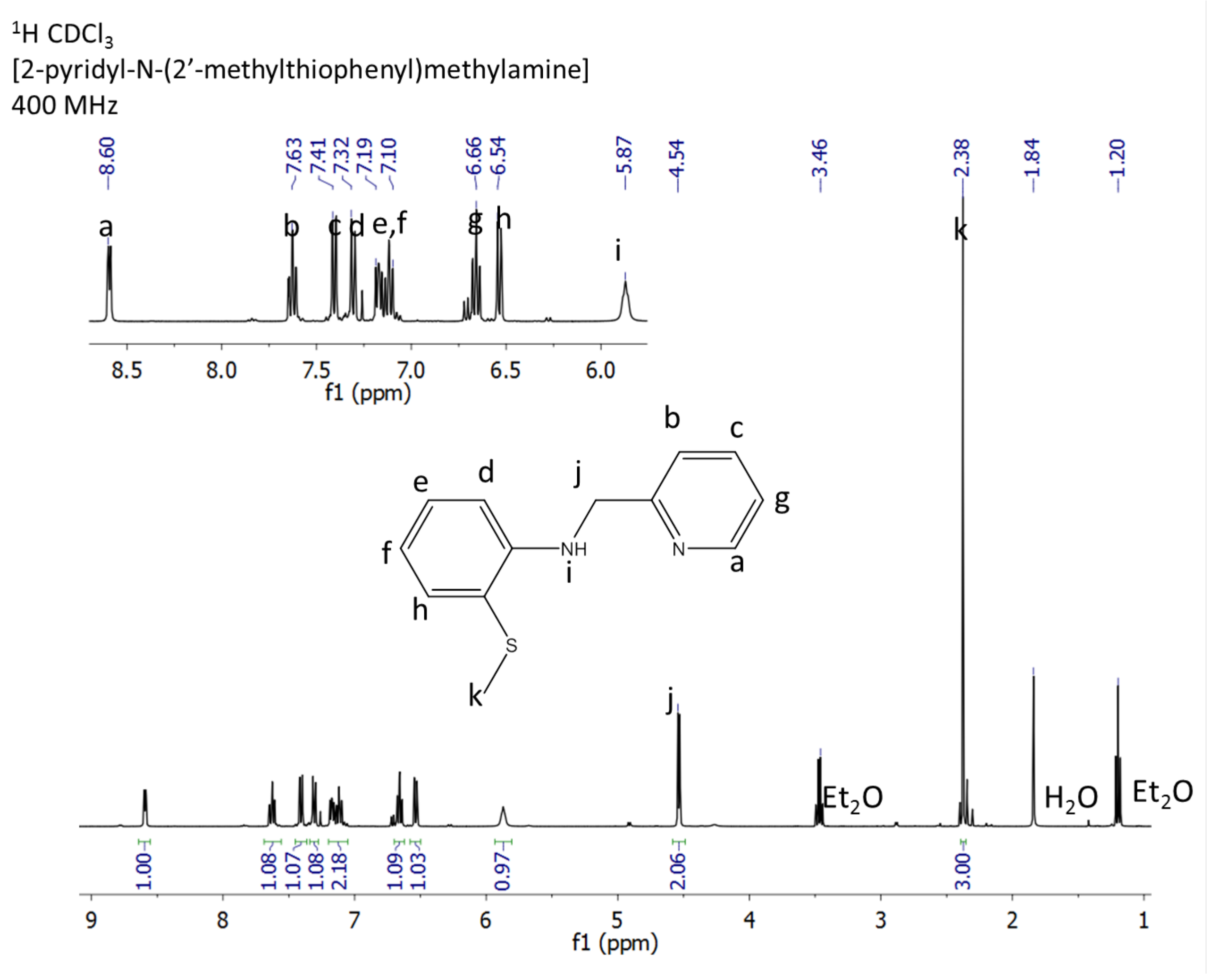

Figure S3. 2-Pyridyl-N-(2'-methylthiophenyl)methylamine NMR in $CDCl_3$ at 400 MHz.

Bulk electrolysis of 1 and hydrogen quantification

Glassy carbon plates were treated in a CH_3CN solution of 0.09 mM **1** and 27.2 eq. CF_3COOH for 480 seconds at –1.75 V vs Fc^+/Fc. Once electrolyzed, they were rinsed in fresh acetonitrile and blotted dry. Treated electrodes were stored under nitrogen until bulk electrolysis experiments. Treated electrodes were immersed in a CH_3CN solution containing 10 mM CF_3COOH and 0.25 M $[Bu_4N][PF_6]$ and the bulk electrolysis cell (Figure S4) sealed before commencing electrolysis. Electrolysis was carried out at –1.4 V for 600 seconds before 1 mL of the gas headspace was removed using a 1.0 mL Vici Pressure-Lok Precision Analytical Syringe. This syringe was used to inject three separate ca. 0.3 mL samples into a Varian 450-GC with a pulsed discharge helium ionization detector and the average integrated hydrogen peak area calculated. A recently recorded calibration curve made from samples of 0.5, 1.0, 3.0, and 5.0 v/v % H_2 in air for this specific instrument[5] was generously provided for our use and used to quantify the volume fraction of hydrogen in the gas aliquot. Using this volume fraction and the measured volume of the headspace, the number of moles of hydrogen was determined. The number of moles of dissolved hydrogen in the working compartment solution was estimated using Henry's Law and added to the number of moles of hydrogen in the headspace to yield a total amount of produced hydrogen. The Henry's Law constant for hydrogen in acetonitrile was estimated to be 5700 atm from literature values for the mole fraction solubility of hydrogen measured at different partial pressures of hydrogen at 298 K.[6] Using the total amount of charge passed during electrolysis the theoretical amount of hydrogen produced was determined and compared with the actual amount of hydrogen produced to find an experimental Faradaic efficiency of approximately 97%.

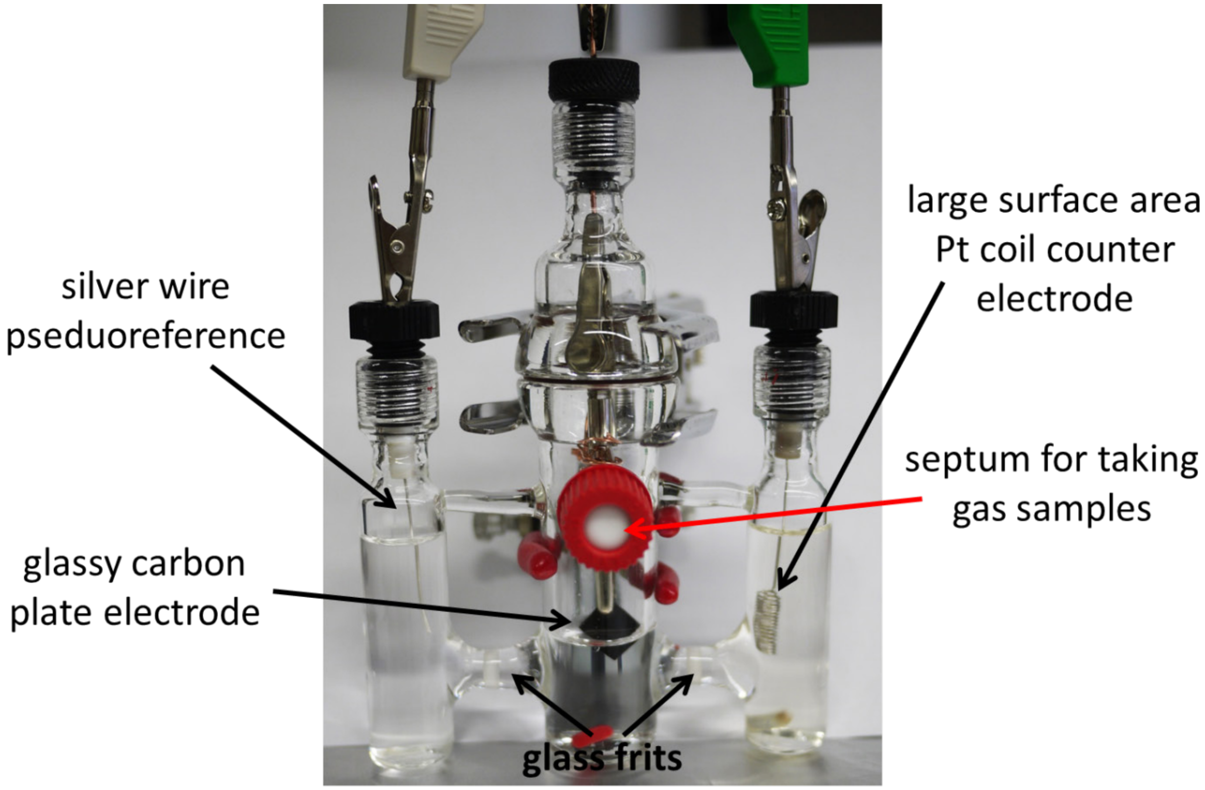

Figure S4. Photo of three-compartment bulk electrolysis cell used to produce hydrogen for detection by bulk electrolysis. Cell was custom made by Allen Scientific Glass, Inc. The Pt coil counter electrode was purchased from BioLogic Science Instruments.

Electrochemistry of 1 and 2 in the absence of acid

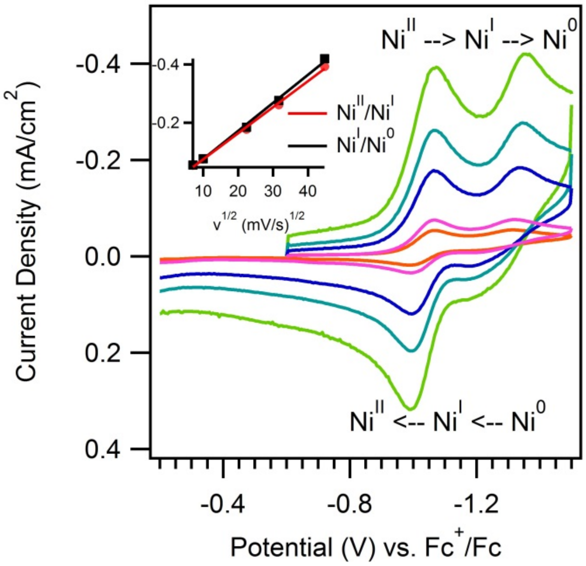

Figure S5. Cyclic voltammograms of 0.2 mM **1** in 100 mM [Bu_4N][PF_6] acetonitrile at varying scan rates of 50, 100, 500, 1000, and 2000 mV/s. Both waves exhibit a linear trend with respect to the square root of the scan rate. The first redox event appears highly reversible, while the second redox event appears quasi-reversible, possibly due to slow ligand reorganization upon oxidation.

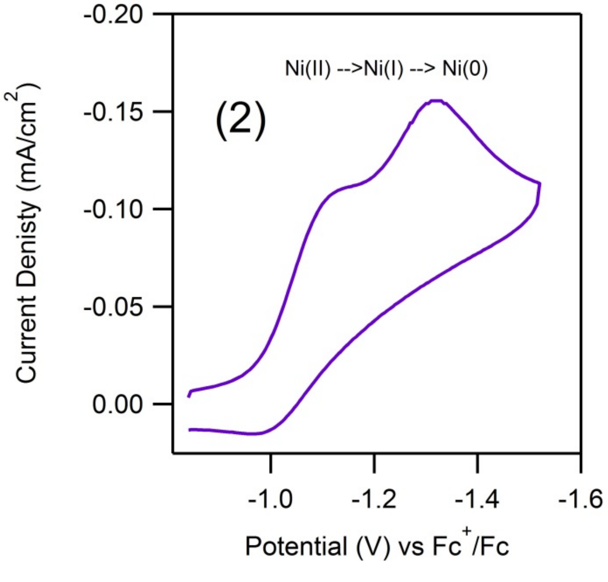

Figure S6. Cyclic voltammogram of 0.39 mM **2** in 100 mM [Bu_4N][PF_6] acetonitrile at 100 mV/s.

Electrochemistry of the 2-pyridyl-N-(2'-methylthiophenyl)methyleneimine ([N-N-SCH_3]) ligand

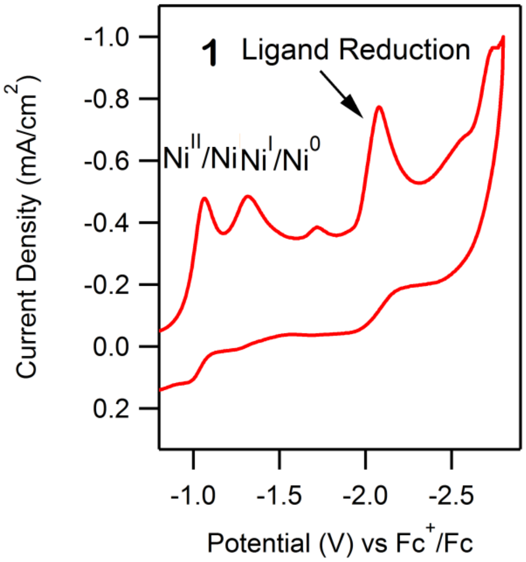

Figure S7. Cyclic voltammogram of 1.7 mM **1**. At approximately –2.0 V vs. Fc^+/Fc, a two electron reduction attributed to direct ligand reduction is observed (see **Figure S8**). A peak at –1.7 V vs. Fc^+/Fc was not assigned. Voltammograms recorded at 100 mV/s in 100 mM $[Bu_4N][PF_6]$ acetonitrile.

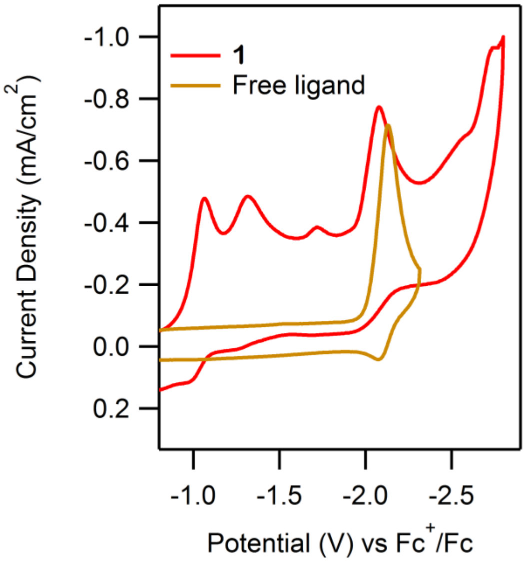

Figure S8. Cyclic voltammograms of 1.7 mM **1**, and 3.4 mM 2-pyridyl-N-(2'-methylthiophenyl)methyleneimine ([N-N-SCH_3]) solutions. The coordinated ligand reduction is positively shifted from the free ligand reduction, but the relative current densities are similar. All voltammograms were recorded at 100 mV/s in 100 mM mM $[Bu_4N][PF_6]$ acetonitrile.

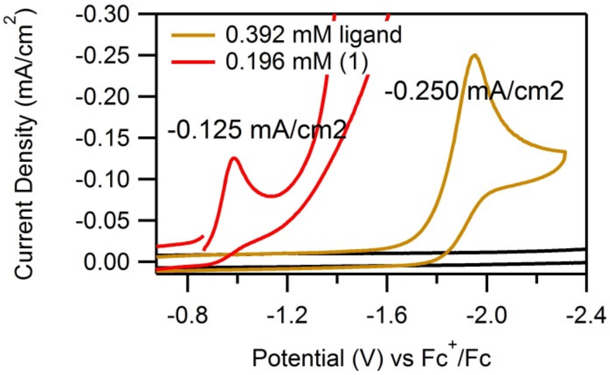

Figure S9. Cyclic voltammograms of a solution of 0.196 mM **1** with 2.6 mM CF_3COOH and a solution of 0.392 mM 2-pyridyl-N-(2'-methylthiophenyl)methyleneimine ([N-N-SCH_3]) with 5.2 mM CF_3COOH. The ligand only solution is twice the concentration of the precatalyst solution, as the precatalyst has two ligands per nickel. In the absence of acid (**Figure S8**), peak integration found that the stoichiometric ratio of prewave : ligand hydrogenation as 1:2, indicating 1 electron per ligand. In the presence of acid, the two electron ligand reduction transforms into a four electron ligand hydrogenation (2 electrons/ligand). All voltammograms were recorded at 100 mV/s in 100 mM mM $[Bu_4N][PF_6]$ acetonitrile.

Peak integrations from CVs of 1

Table S1. Peak integrations of the prewave of **1**, ligand reduction, and direct ligand hydrogenation relative to the Ni^{II}/Ni^{I} reduction. As noted in **Figure S8** and **Figure S9**, the concentration of ligand for direct ligand reduction and hydrogenation peak integration was twice that of the concentration of **1**, as required of the complex being ligated by two ligands.

	Ni^{II}/Ni^{I}	Direct Ligand Reduction	Direct Ligand Hydrogenation	Prewave
# e^- passed	1.00	1.92	4.08	2.99*

*The prewave integration is a combination of the two electron ligand hydrogenation and a single electron Ni^{II}/Ni^{I} reduction.

Prewave peak height analysis

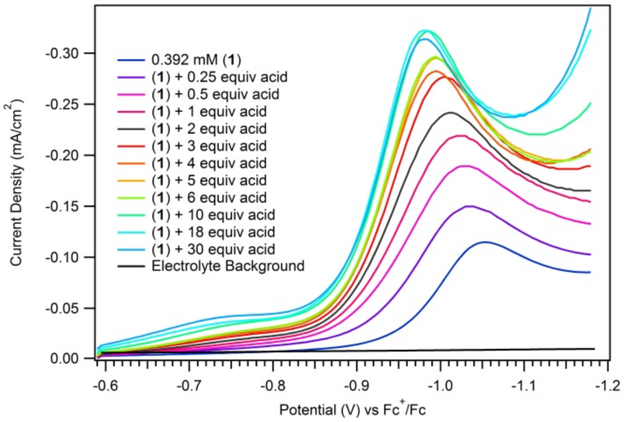

Figure S10. Peak heights of the prewave, relative to the peak height of the first reduction for acid-free samples of **1**, were calculated using the above voltammograms produced with 0.39 mM **1** and subsequent additions of trifluoroacetic acid. Electrodes were scanned cathodically and stopped before the catalytic wave to avoid contribution to the peak height from the catalytic wave onset. All scans were conducted in 100 mM $[Bu_4N][PF_6]$ acetonitrile at 100 mV/s.

Direct reduction of $[CF_3COOH]$ vs. 1 + acid

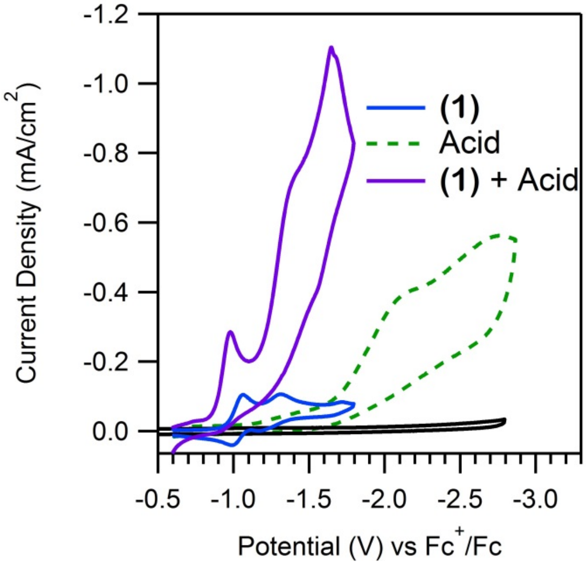

Figure S11. Cyclic voltammograms of 0.38 mM **1** with and without 7.2 equiv of $[CF_3COOH]$, as well as an acid-only background of equal concentration. All scans at 100 mV/s in 100 mM $[Bu_4N][PF_6]$ acetonitrile solution.

Electrochemistry of 1 and iodine free 1

In **1**, a trace iodine contamination was present after synthetic workup (as detected by elemental analysis), a byproduct of ligand methylation via MeI. We suspected that I$^-$ acted as a counter anion (in place of $[BF_4]^-$) for a subset of molecules in samples of **1**. A more rigorous workup was performed to remove iodine from a separate batch of **1** (as described in the synthetic procedure above), and the electrochemistry of the two samples were compared, below.

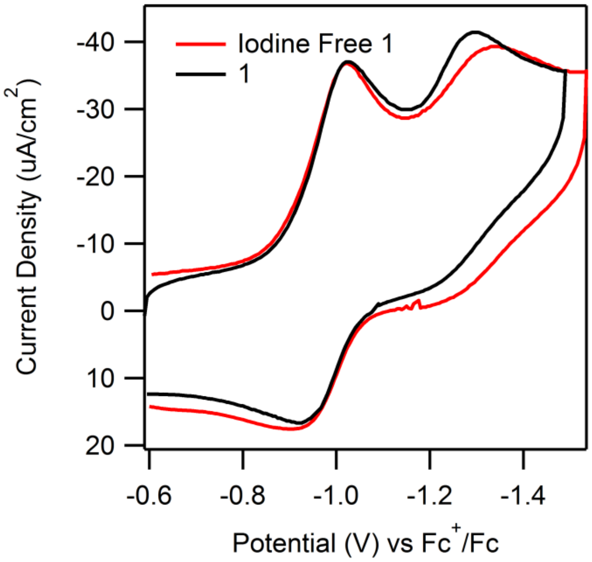

Figure S12. Cyclic voltammograms of 0.08 mM **1** and **1** without iodine contamination. All scans at 100 mV/s in 100 mM $[Bu_4N][PF_6]$ acetonitrile solution.

Absorption spectra 1 and 2 upon acid titrations

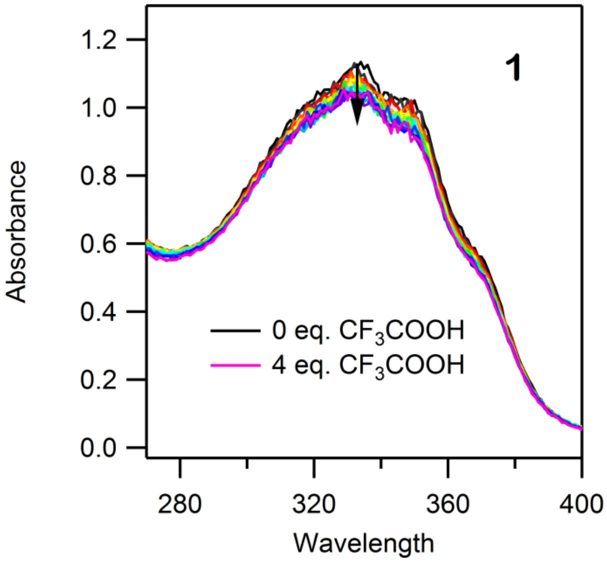

Figure S13. Absorption spectra of **1** upon additions of acid aliquots. No change is observed other than dilution of the sample upon acid addition.

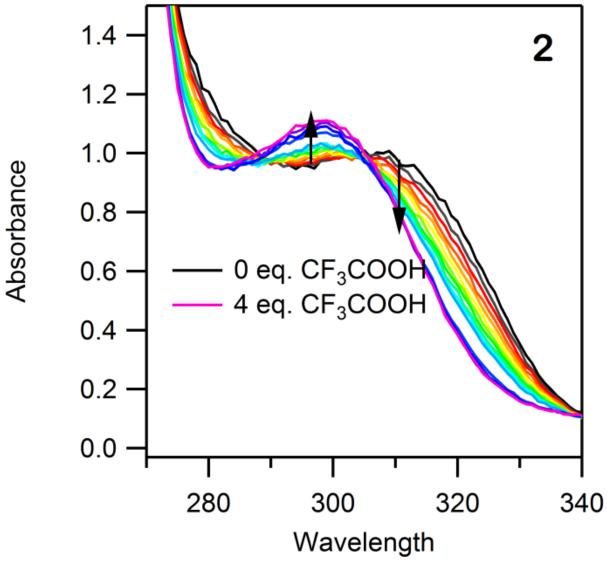

Figure S14. Absorption spectra of **2** upon additions of trifluoroacetic acid aliquots**.** Protonation leads to a new species with absorbance that is blue-shifted relative to the absorbance of **2**. Two isosbestic points are observed as the absorbance of the newly generated species approaches a maximum. This reversible process (see **Figure S15**) is attributed to protonation of the sp^3 hybridized nitrogens in the ligand backbone of **2**.

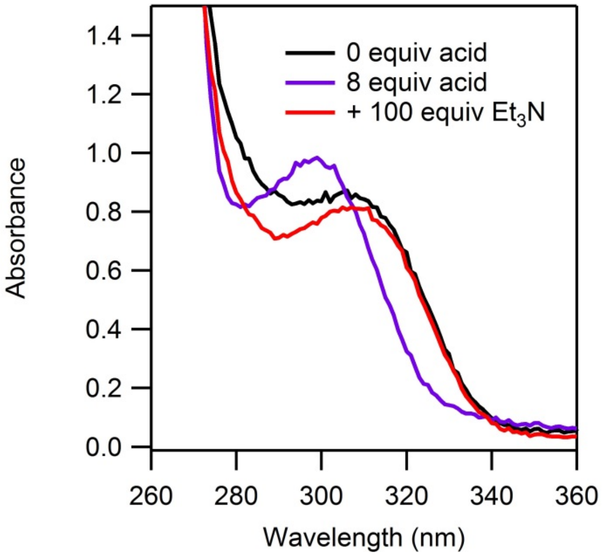

Figure S15. Upon protonation of **2** with trifluoroacetic acid, addition of Et_3N regenerates the original absorbance features of **2**. Coordination of triethylamine may account for the change between starting and ending spectra.

Acid titrations of trifluoroacetic acid into solution of 1 and acid.

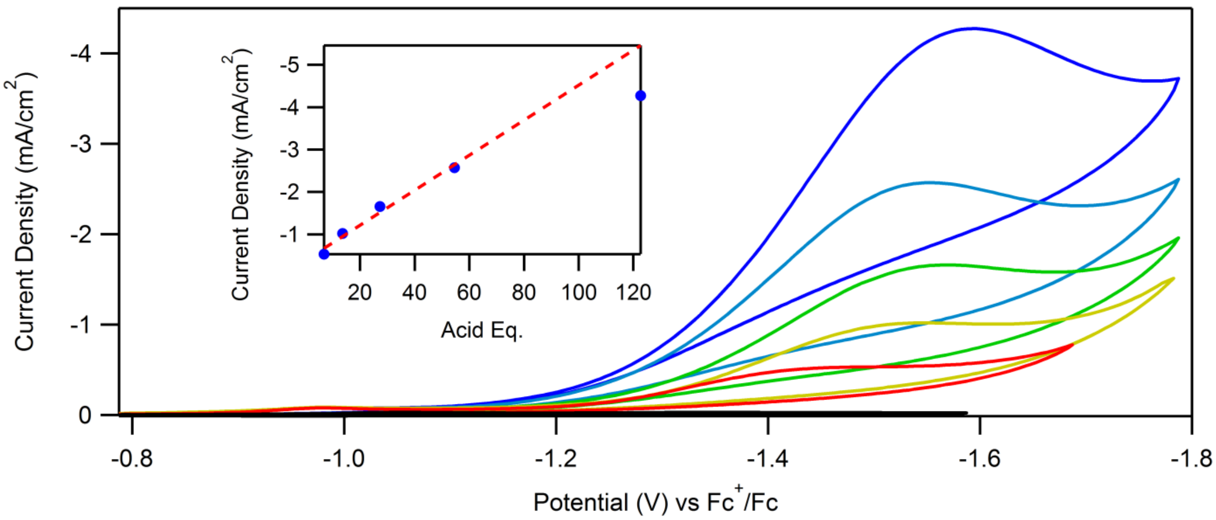

Figure S16. Cyclic voltammograms of a solution of **1** (0.096 mM) with acid additions of 6.8, 13.6, 27.3, and 54.5 eq. of CF_3COOH. All voltammograms were recorded at 100 mV/s in 100 mM $[Bu_4N][PF_6]$ acetonitrile solution. Inset: The dashed linear line was fit to the peak intensities of the catalytic wave for acid titrations up to 55 equivalents.

Rinse Test for 1

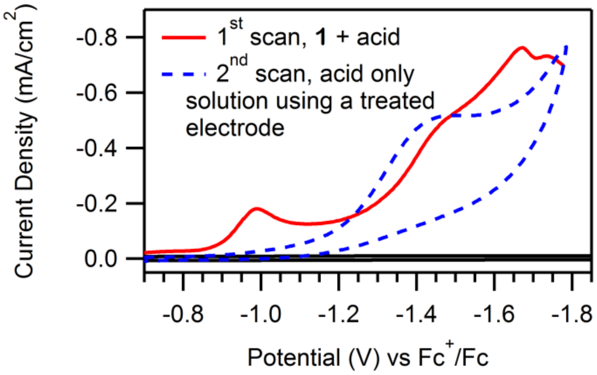

Figure S17. In the acidic solution of **1** (0.20 mM **1**, 13.6 eq. CF_3COOH), produced a voltammogram with both a prewave and catalytic current (red trace). When the electrode was removed, rinsed, and placed in an acid-only solution of equal concentration, no prewave was observed in the resulting voltammogram (dashed blue trace). The positive shift reflects the time dependence of the film generation. The black trace is of the untreated electrode background. Voltammograms recorded at 100 mV/s in 100 mM $[Bu_4N][PF_6]$ CH_3CN solutions.

Potential and time dependence on deposition conditions of 1

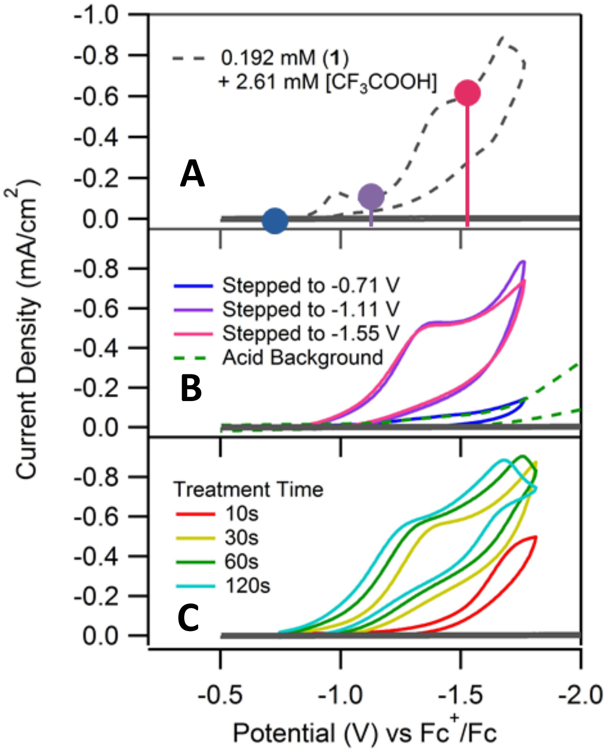

Figure S18. A) Cyclic voltammogram of a solution of **1** and acid and catalyst. B) Over varying potential ranges, individual electrodes were treated in solutions of the acid and catalyst. Once treated for 180 seconds, each was rinsed with acetonitrile before being submerged in an acid-only solution of equal concentration. C) At a single potential beyond the prewave (–1.16 V), varying treatment times were applied to different electrodes. Each was then scanned in an acid-only solution. All cyclic voltammograms were recorded at 100 mV/s in 100 mM [Bu_4N][PF_6] acetonitrile solution

To evaluate deposition conditions more closely, potential steps of varying magnitude were applied to a series of freshly polished electrodes in an acidic solution of **1** before the 'treated' electrodes were thoroughly rinsed with CH_3CN and submerged in fresh, acid-only solutions. When stepped to potentials prior to the pre-wave in the acidic **1** solution, the treated electrodes produced voltammograms indistinguishable from the acid-only background. When stepped to potentials more negative than that of the pre-wave, voltammograms of the treated electrodes in the acid-only solution produced catalytic waves similar to that observed in the acidic **1** solution. Increasing the time of the potential step correlates with a positive shift of the catalytic wave onset potentials for the electrodeposited film in the acid-only solution, yet did not affect the current observed.

Acid titrations of trifluoroacetic acid into acid only solutions using electrode treated with 1

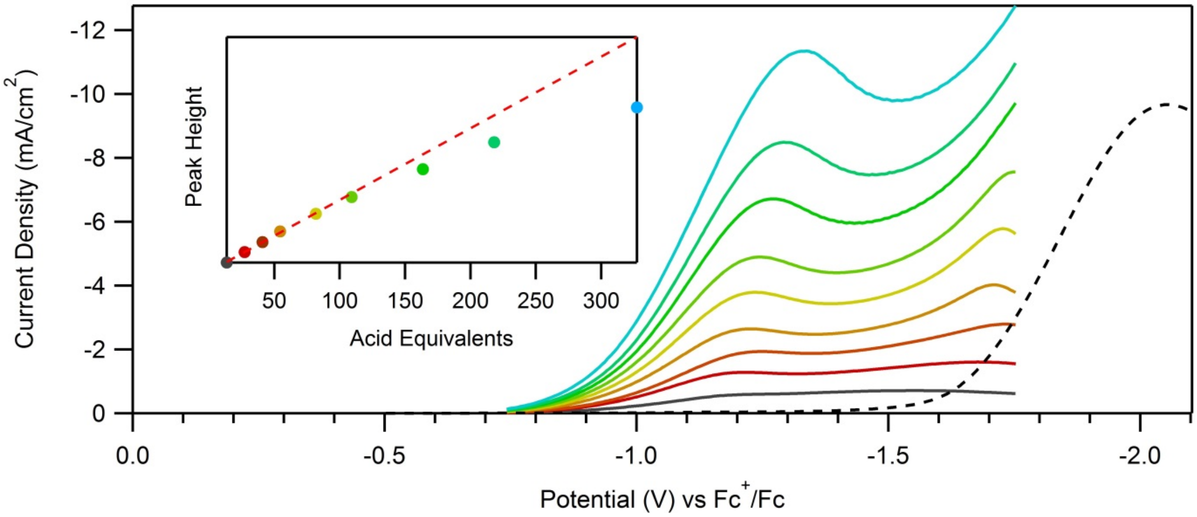

Figure S19. An electrode treated for 480 s in an acidic solution of 0.19 mM **1** produced these voltammograms in an acid-only solution with subsequent acid titrations. All voltammograms were produced at 100 mV/s in 100 mM [Bu_4N][PF_6] acetonitrile solution. Inset: The dashed linear fit line was produced using the peak intensities of the catalytic wave for acid titrations up to 80 equivalents.

Rinse Test of 2

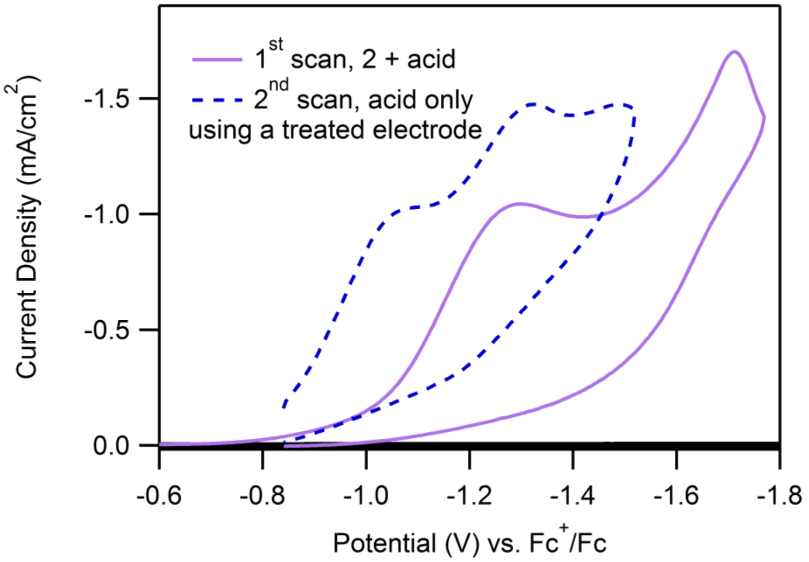

Figure S20. In the acidic solution of **2** (0.39 mM **2**, 13.6 eq. CF_3COOH), the purple trace was recorded. A separate electrode was treated for 480 s at –1.2 V in this solution, rinsed, and placed in an acid-only solution of equal concentration, yielding the dashed blue trace. The positive shift reflects the time dependence of the film generation. The black trace is of the untreated electrode background. Voltammograms recorded at 100 mV/s in 100 mM [Bu_4N][PF_6] acetonitrile solutions.

Modification of glassy carbon and platinum electrodes

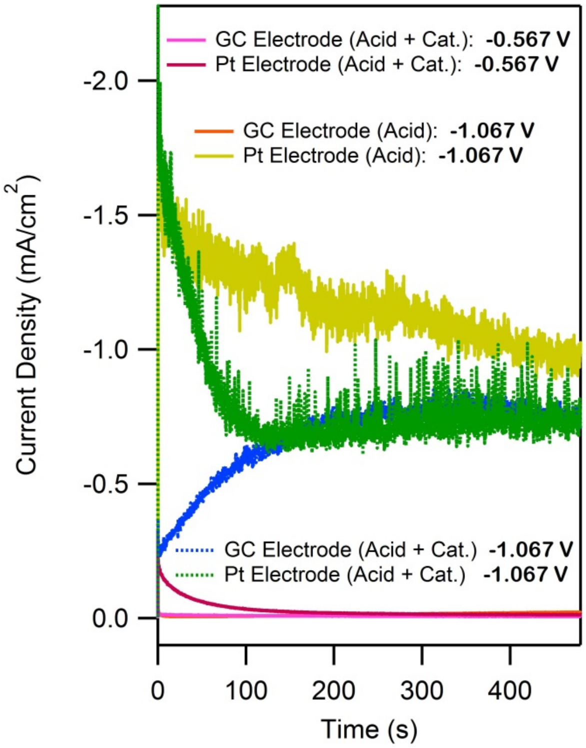

Figure S21. Chronoamperograms of both glassy carbon and platinum under a variety of conditions. Single glassy carbon and platinum electrodes were held at potentials beyond the prewave in acid-only solutions (orange and yellow). The yellow line decreases linearly as the bulk concentration of protons in solution was changed. Single glassy carbon and platinum electrodes were held at potentials prior to the prewave in a solution of 0.19 mM (**1**) and 2.6 mM [CF_3COOH] for 480 s (pink and red). The glassy carbon electrode under these conditions produced a chronoamperogram indistinguishable from that of the acid-only glassy carbon chronoamperogram. The platinum electrode under these conditions produced a decaying plot, corresponding to the depletion of protons to the electrode. Finally, glassy carbon and platinum electrodes were held at potentials beyond the prewave in the same catalyst and acid solution as before for 480 s (blue and green), which leveled out to the same current density.

Chronoamperograms of rapidly stirring acidic solutions of **1** employing either a glassy carbon or platinum electrode result in constant current responses when the applied potential is more positive than the prewave. At more negative potentials, the current at a glassy carbon electrode increases over time, asymptotically approaching an upper limit. By contrast, a platinum working electrode under identical conditions exhibited the opposite trend; the current decreased over time, asymptotically approaching a lower limit. After correcting the current densities to reflect the relative surface areas, the two limiting current values were indistinguishable. For both electrodes the generation of active material occurs after an induction period, suggesting heterogeneous catalysis formation from homogeneous molecular catalysts.[7] The current plateaus as the percent 'untreated' surface area diminishes as the electrodeposited film forms.

Observation that an identical limiting current is reached for both electrodes during the chronoamperometry measurement indicates that an active material is deposited onto the electrode surfaces. For glassy carbon, this electrodeposited material is a 'better' proton reduction catalyst than the unmodified electrode.[8] For the case of platinum, an already efficient proton-reduction catalyst, depositing the active material obscures the more active electrode material.

SEM and TEM Images of Electrolyzed 1 and 2

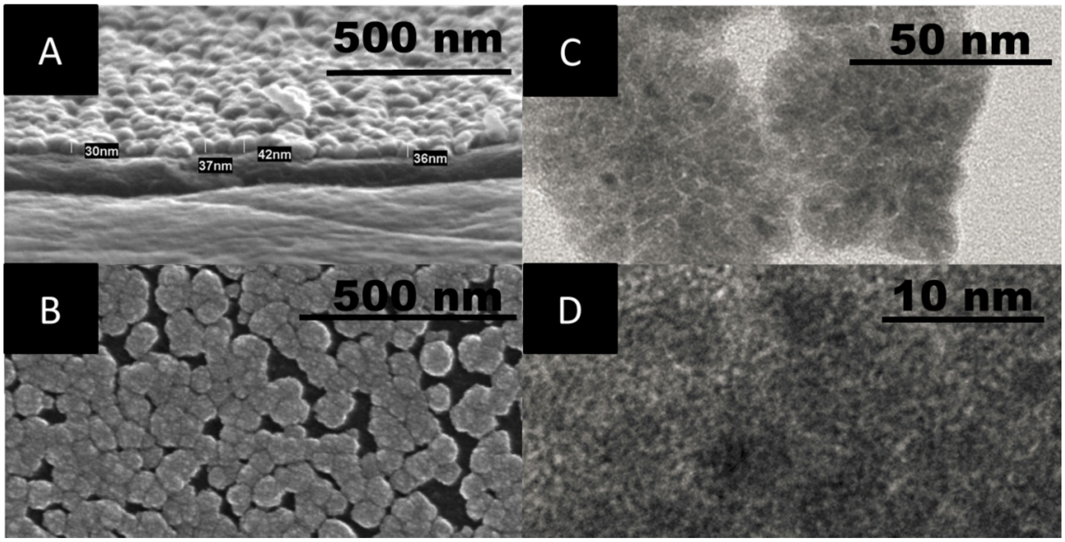

Figure S22. Images of glassy carbon plates electrolyzed in 0.19 mM **1** and 13.6 eq. CF_3COOH for 480s at –1.75 V. TEM images obtained by scraping the film off a treated glassy carbon plate, suspending the material in EtOH, and drop casting on TEM grids. (A) SEM cross-section profile of the deposited film. (B) A top-down view of the film. (C) TEM micrograph showing nanoparticles (dark areas). (D) High resolution TEM of single nanoparticles.

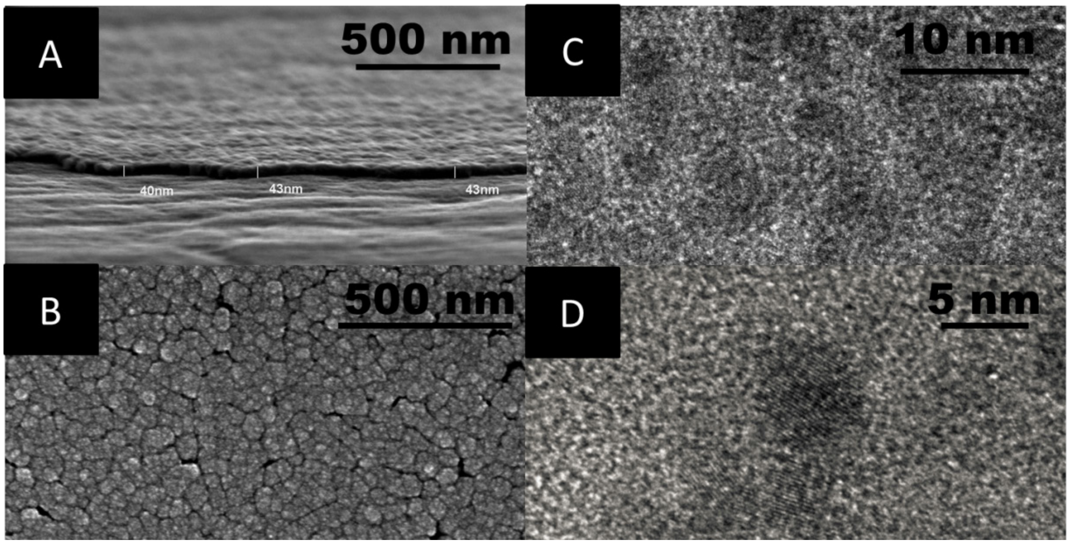

Figure S23. Images of glassy carbon plates electrolyzed in 0.19 mM **2** and 13.6 eq. CF_3COOH for 480s at –1.75 V. TEM images obtained by scraping the film off a treated glassy carbon plate, suspending the material in EtOH, and drop casting on TEM grids. (A) SEM cross-section profile of the deposited film. (B) A top-down view of the film. (C) TEM micrograph showing nanoparticles (dark areas). (D) High resolution TEM of a single nanoparticle, revealing a crystalline structure.

Anodic Stripping of Ni^0 from Treated Electrodes

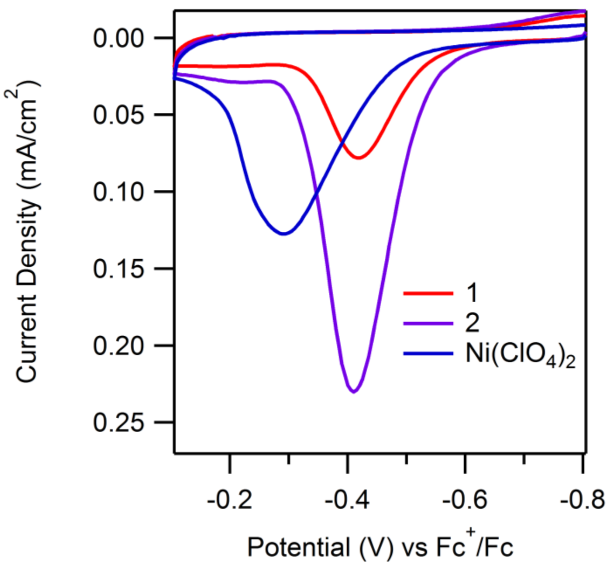

Figure S24. Stripping waves produced by single voltammograms of solutions of 0.19 mM **1**, **2**, or $Ni(ClO_4)_2$ and CF_3COOH (13.6 eq.). Voltammograms were recorded at 100 mV/s in 100 mM $[Bu_4N][PF_6]$ acetonitrile solution.

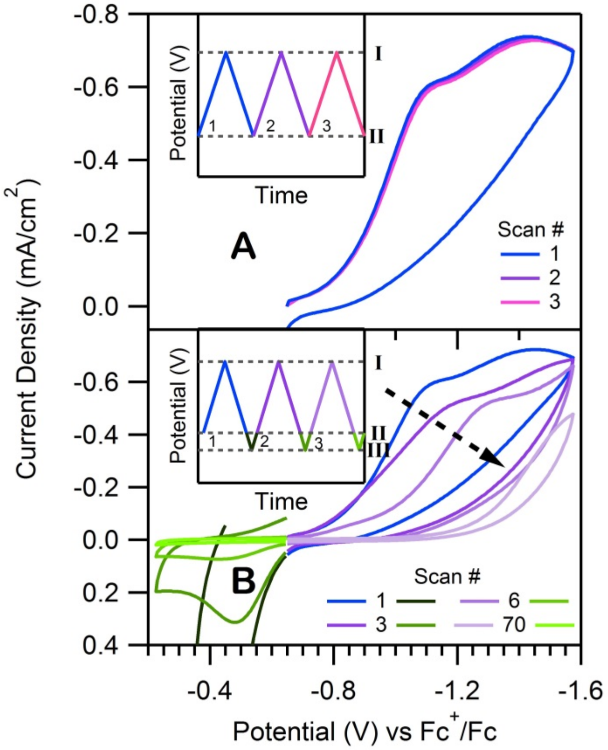

Figure S25. A treated electrode was generated from 0.19 mM **1** and 2.5 mM trifluoroacetic acid, rinsed, and transferred to an equimolar acid only solution where it was then evaluated using one of two conditions. Condition (A): the acid only solution was stirred between scans and the scanned potential window is limited to potentials negative of the nickel stripping wave. When (A) is satisfied, little difference in the voltammograms is observed on repeated scans. Condition (B): the acid only solution was stirred between scans, but the switching potential positive of the nickel stripping wave (–0.65 V vs. Fc^+/Fc). When (B) is met, catalytic current decreases and the onset shifts negatively upon successive scans. All voltammograms recorded at 100 mV/s in 100 mM $[Bu_4N][PF_6]$ acetonitrile solution.

Comparison of $Ni(ClO_4)_2 \cdot 6H_2O$ vs. 1 vs. 2 precatalysts

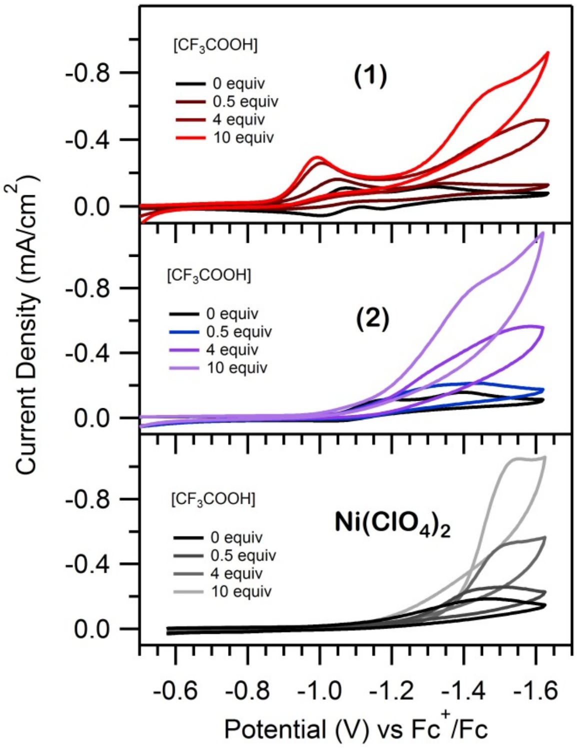

Figure S26. Voltammograms of acid titrations of $[CF_3COOH]$ into 0.39 mM, solutions of (**1**), (**2**), or $Ni(ClO_4)_2$. Catalysis is apparent in all three situations. No prewave is observed for 2 or $Ni(ClO_4)_2$. The onset potential of catalysis from solutions of $Ni(ClO_4)_2$ is more negative than that of either **1** or **2**. All scans were taken at 100 mV/s in 100 mM $[Bu_4N][PF_6]$ acetonitrile solution.

As the electrodeposition of Ni^0 continues throughout the CV for solutions of $Ni(ClO_4)_2$, curve crossing of the catalytic wave is observed on the reverse scan. More catalytically active material is present on the return trace, so higher hydrogen evolution rates may occur.

XPS spectra and analysis

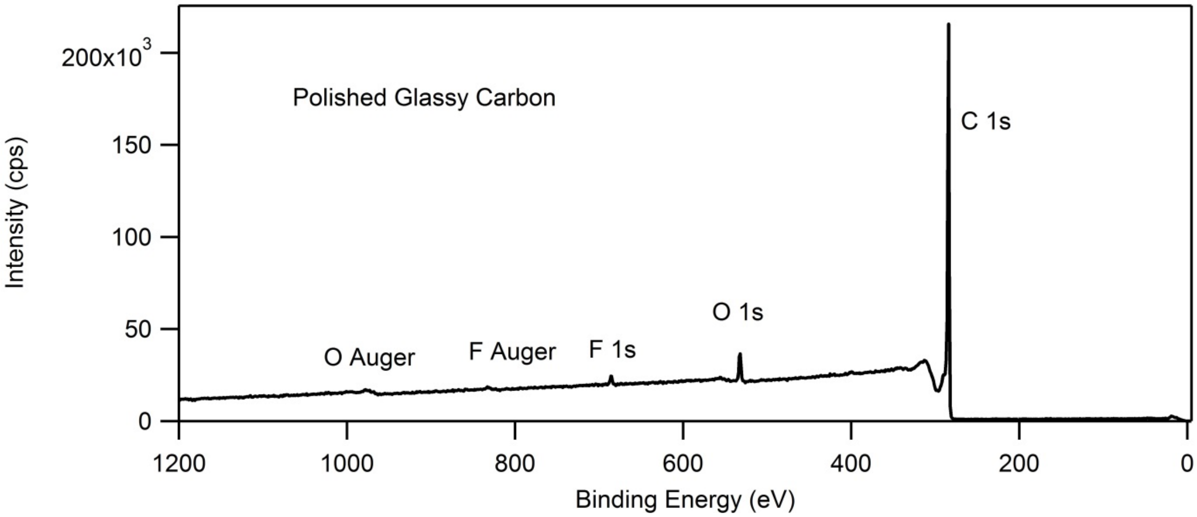

Figure S27. Full spectrum of a polished glassy carbon plate subjected to no additional treatment beyond polishing and rinsing.

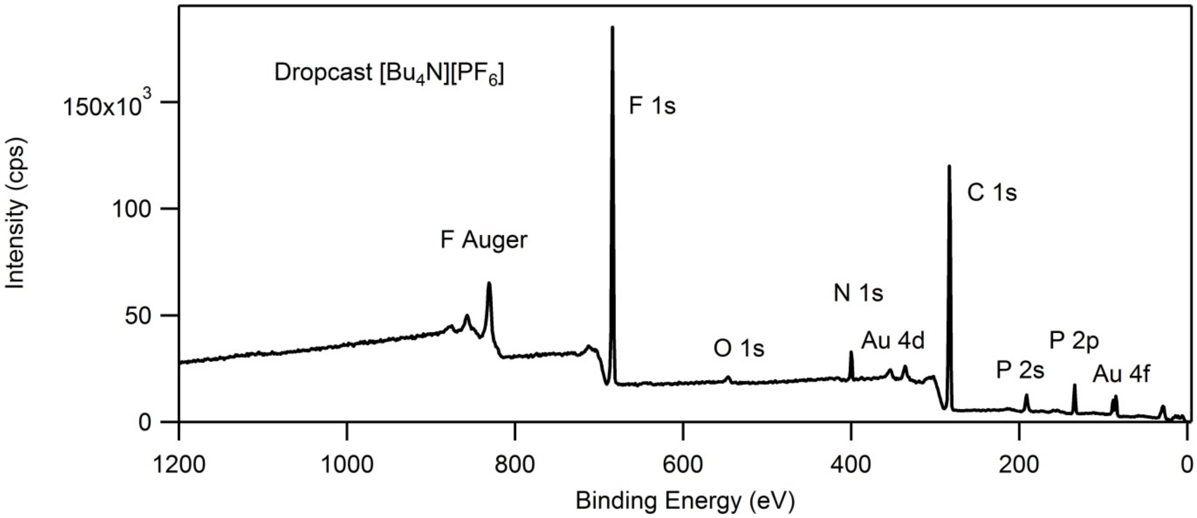

Figure S28. Full spectrum of dropcast $[Bu_4N][PF_6]$ onto a gold plated silica wafer.

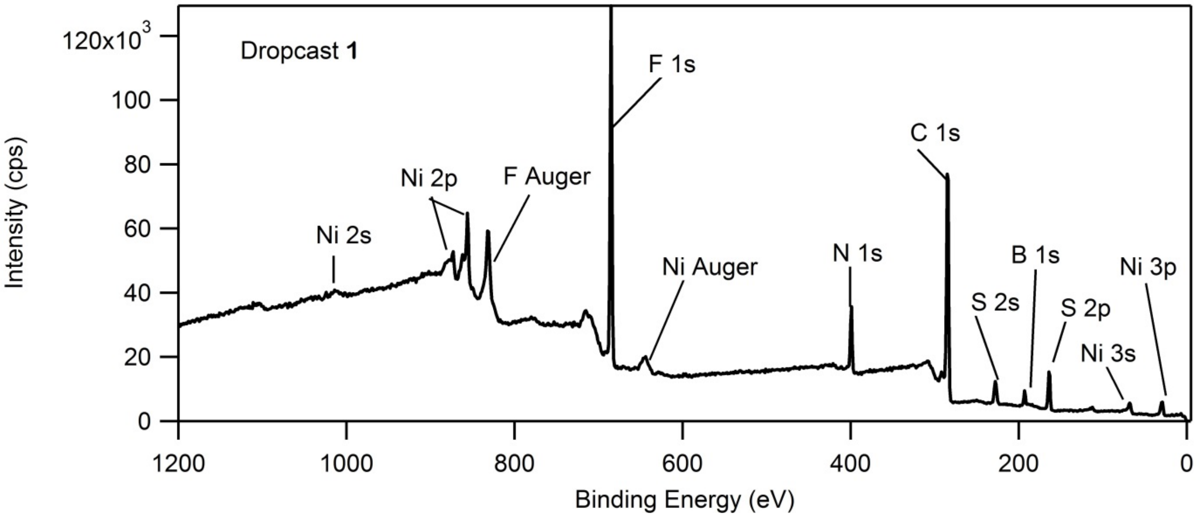

Figure S29. Full spectrum of dropcast **1** onto a gold plated silica wafer.

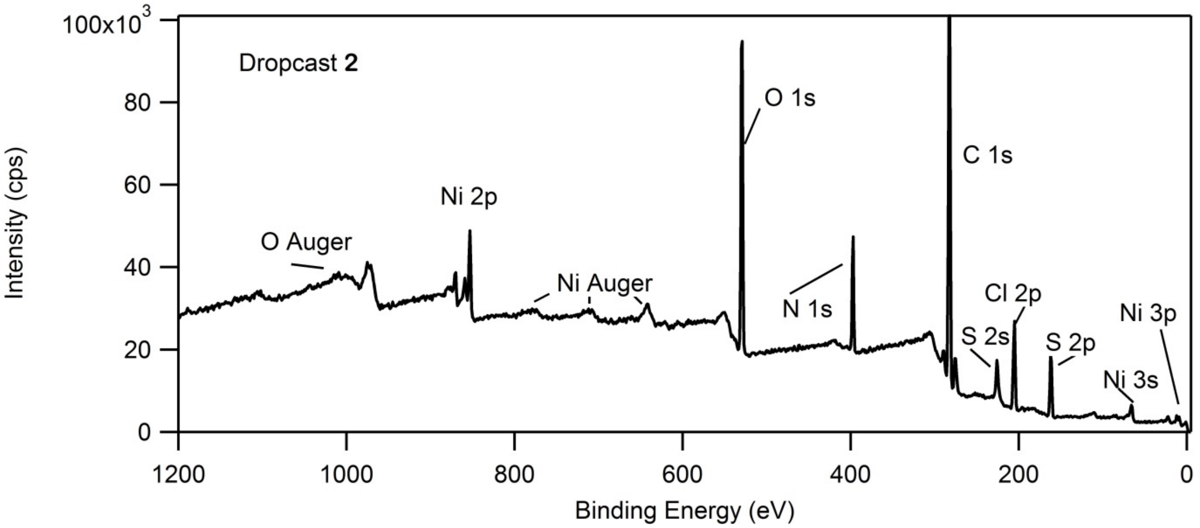

Figure S30. Full spectrum of a dropcast sample of **2** onto a gold plated silica wafer.

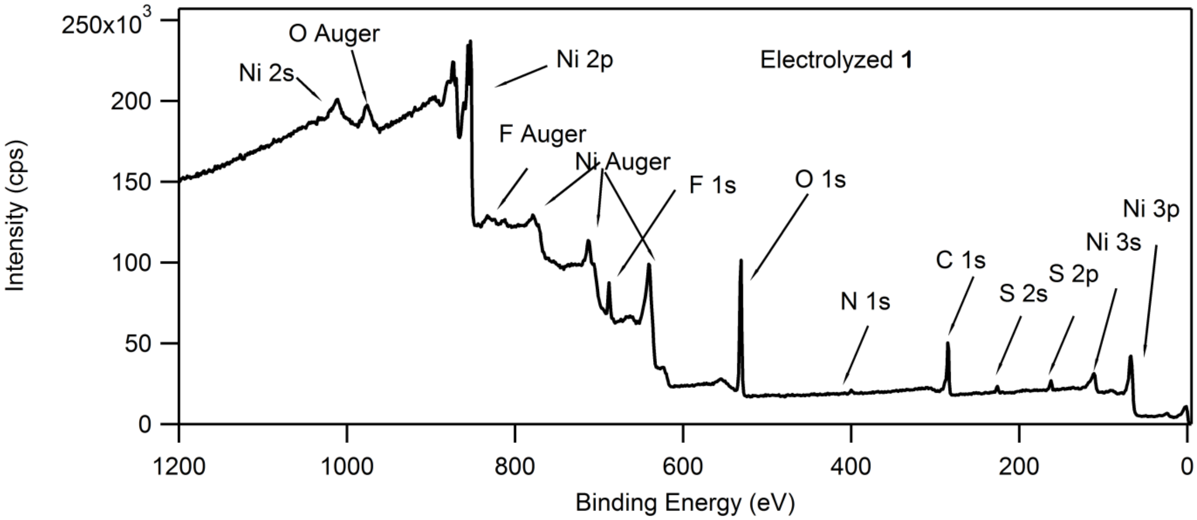

Figure S31. Full spectrum of electrolyzed glassy carbon plate from a solution of 0.192 mM **1** and 13.63 eq. CF_3COOH for 480 seconds.

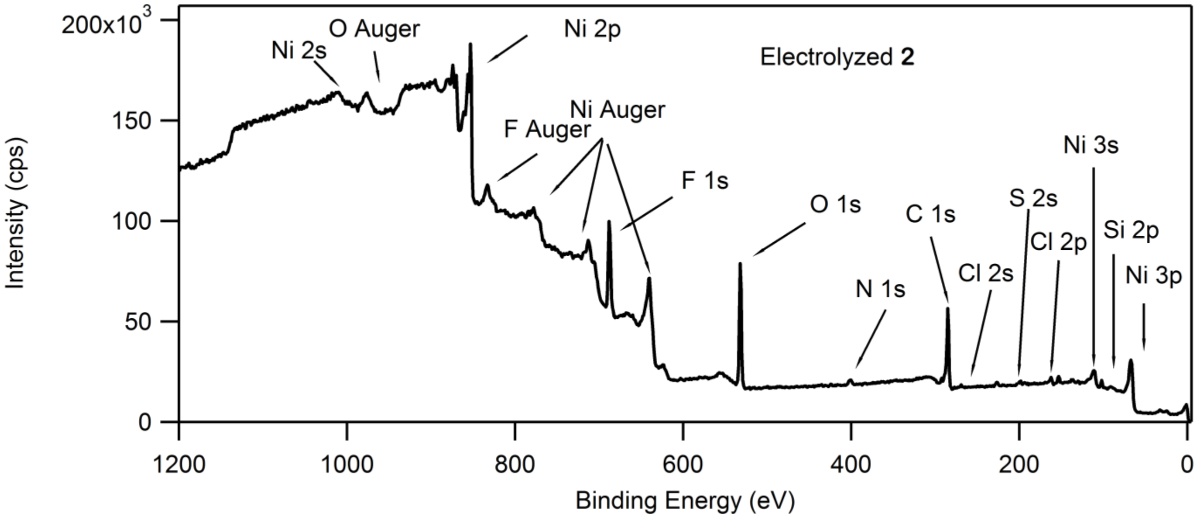

Figure S32. Full spectrum of an electrolyzed sample of glassy carbon plate electrolyzed in a 0.192 mM **2** and 13.63 eq. CF_3COOH solution for 480 seconds.

Table S2. XPS elemental analysis summary of atomic ratio percentages. Samples include: Dropcast **1,** electrolyzed glassy carbon plate from a solution of 0.192 mM **1** and 13.63 eq. CF_3COOH for 480 seconds, dropcast **2**, electrolyzed glassy carbon plate from a solution of 0.192 mM **2** and 13.63 eq. CF_3COOH for 480 seconds, polished glassy carbon plate, and dropcast $[Bu_4N][PF_6]$. For both electrolyzed **1** and **2**, the relative contribution of Ni metal in the Ni 2p signal was calculated by fitting the Ni metal with a doublet (Ni $2p_{3/2}$ peak position of 852.8 eV and a peak separation of 17.27 eV).

Peak	Dropcast **1**	Electrolyzed **1**	Dropcast **2**	Electrolyzed **2**	Glassy Carbon Plate	Dropcast $[Bu_4N][PF_6]$
Ni 2p	2.72	20.17	1.78	8.63	-	-
Ni 2p Ni^0	-	5.52	-	4.51	-	-
N 1s	7.96	1.17	9.28	2.37	0.63	4.33
S 2p	4.03	2.71	3.95	1.51	0.14	0.35
C 1s	58.85	35.46	63.80	44.87	95.33	65.17
B 1s	5.19	0.86	-	-	-	-
F 1s	21.24	5.48	-	14.80	0.78	24.36
O 1s	-	28.64	16.93	22.47	3.11	2.29
P 2p	-	0.00	0.00	0.00	0.00	3.50
Cl 2p	-	-	4.26	0.84	-	-

Table S3. Theoretical vs. experimental XPS elemental analysis. All atomic ratio percentages are normalized to the percentage of Ni 2p in respective samples.

Peak	Theoretical **1**	Dropcast **1**	Electrolyzed **1**	Theoretical **2**	Dropcast **2**	Electrolyzed **2**
Ni 2p	1.00	1.00	1.00	1.00	1.00	1.00
N 1s	4.00	2.93	0.05	4.00	5.21	0.18
S 2p	2.00	1.48	0.11	2.00	2.22	0.12

TEM-EDS analysis

Sample were prepared for TEM analysis by electrolyzed 0.19 mM **1** or **2** for 480 seconds at –1.75 V with 13.6 eq. CF_3COOH using a glassy carbon. The resulting thin film was scraped off the glassy carbon plate and suspended in ethanol before being dropcast onto a copper matrix for analysis.

Table S4. EDS elemental analysis results for electrolyzed **1**.

Element	Weight%	Weight% Sigma	Atomic%
C K	12.22	0.14	38.00
O K	3.16	0.08	7.39
Si K	0.21	0.03	0.28
S K	2.23	0.04	2.59
Cl K	0.24	0.03	0.26
Ni K	73.94	0.16	47.04
Cu K	7.12	0.08	4.19
I L	0.87	0.06	0.26
Totals	100.00		

Table S5. EDS analysis of electrolyzed sample of **2**.

Element	Weight%	Weight% Sigma	Atomic%
C K	7.40	0.46	26.01
O K	2.77	0.28	7.31
S K	2.98	0.19	3.92
Cl K	1.61	0.15	1.92
Ni K	77.52	0.59	55.72
Cu K	7.71	0.35	5.12
Totals	100.00		

References

1. L. I. Lindoy, S. E. Livingstone, and T. N. Lockyer, 1965, 1549–1560.

2. L. F. Lindoy and S. E. Livingstone, *Inorg. Chem.*, 1968, **7**, 1149–1154.

3. S. K. Chatterjee, S. Roy, S. K. Barman, R. C. Maji, M. M. Olmstead, and A. K. Patra, *Inorg. Chem.*, 2012, **51**, 7625–35.

4. G. R. Fulmer, A. J. M. Miller, N. H. Sherden, H. E. Gottlieb, A. Nudelman, B. M. Stoltz, J. E. Bercaw, and K. I. Goldberg, *Organometallics*, 2010, **29**, 2176–2179.

5. C. L. Pitman and A. J. M. Miller, *ACS Catal.*, 2014, **4**, 2727–2733.

6. E. Brunner, *J. Chem. Eng. Data*, 1985, **30**, 269–273.

7. J. A. Widegren and R. G. Finke, *J. Mol. Catal. A Chem.*, 2003, **198**, 317–341.

8. B. D. McCarthy, D. J. Martin, E. S. Rountree, A. C. Ullman, and J. L. Dempsey, *Inorg. Chem.*, 2014, **53**, 8350–61.

9. D. L. Reger and C. Coleman, *J. Organomet. Chem.*, 1977, **131**, 153–162.